8-1-2012

Understanding the in vivo Uptake Kinetics of a Phosphatidylethanolamine-binding Agent ^{99m}Tc-Duramycin

Said H. Audi
Marquette University, said.audi@marquette.edu

Zhixin Li
Medical College of Wisconsin

Joseph Capacete
Marquette University

Yu Liu
Medical College of Wisconsin

Wei Fang
Cardiovascular Research Institute - Fuwai Hospital

See next page for additional authors

Accepted version. *Nuclear Medicine and Biology*, Vol. 39, No. 6 (August 2012): 821-825. DOI.

Understanding the in vivo uptake kinetics of a phosphatidylethanolamine-binding agent ^{99m}Tc-Duramycin

Said Audi
Department of Biomedical Engineering, Marquette University
Milwaukee, WI
Zablocki VA Medical Center
Milwaukee, WI
Division of Pulmonary and Critical Care Medicine, Medical College of Wisconsin
Milwaukee, WI

Zhixin Li
Department of Biophysics, Medical College of Wisconsin
Milwaukee, WI

Joseph Capacete
Department of Biomedical Engineering, Marquette University
Milwaukee, WI

Yu Liu
Department of Biophysics, Medical College of Wisconsin
Milwaukee, WI

Nuclear Medicine and Biology, Vol. 39, No. 6 (August 2012): pg. 821-825. DOI.

Wei Fang
Cardiovascular Research Institute,
Fuwai Hospital, Beijing, China

Laura G. Shu
Department of Biophysics, Medical College of Wisconsin
Milwaukee, WI

Ming Zhao
Department of Biophysics, Medical College of Wisconsin
Milwaukee, WI
Feinberg Cardiovascular Research Institute, Department of Medicine, Northwestern University
Chicago, IL

Abstract:

Introduction

^{99m}Tc-Duramycin is a peptide-based molecular probe that binds specifically to phosphatidylethanolamine (PE). The goal was to characterize the kinetics of molecular interactions between ^{99m}Tc-Duramycin and the target tissue.

Methods

High level of accessible PE is induced in cardiac tissues by myocardial ischemia (30 min) and reperfusion (120 min) in Sprague Dawley rats. Target binding and biodistribution of ^{99m}Tc-duramycin was captured using SPECT/CT. To quantify the binding kinetics, the presence of radioactivity in ischemic versus normal cardiac tissues was measured by gamma counting at 3, 10, 20, 60 and 180 min after injection. A partially inactivated form of ^{99m}Tc-Duramycin was analyzed in the same fashion. A compartment model was developed to quantify the uptake kinetics of ^{99m}Tc-Duramycin in normal and ischemic myocardial tissue.

Nuclear Medicine and Biology, Vol. 39, No. 6 (August 2012): pg. 821-825. DOI.

Results

^{99m}Tc-duramycin binds avidly to the damaged tissue with a high target-to-background radio. Compartment modeling shows that accessibility of binding sites in myocardial tissue to ^{99m}Tc-Duramycin is not a limiting factor and the rate constant of target binding in the target tissue is at 2.2 ml/nmol/min/g. The number of available binding sites for ^{99m}Tc-Duramycin in ischemic myocardium was estimated at 0.14 nmol/g. Covalent modification of D15 resulted in a 9 fold reduction in binding affinity.

Conclusion

^{99m}Tc-Duramycin accumulates avidly in target tissues in a PE-dependent fashion. Model results reflect an efficient uptake mechanism, consistent with the low molecular weight of the radiopharmaceutical and the relatively high density of available binding sites. These data help better define the imaging utilities of ^{99m}Tc-Duramycin as a novel PE-binding agent.

Keywords: ^{99m}Tc-Duramycin, phosphatidylethanolamine, imaging agent.

INTRODUCTION

The asymmetrical distribution of phospholipids in cellular membranes is of fundamental importance [1,2]. The status of this asymmetry has been increasingly recognized as a molecular marker for normality and diseases.

A number of imaging agents have been described in pursuit of targeted imaging capabilities for membrane phospholipids. Annexin V, the C2A domain of Synaptotagmin I, and the C2 domain of Lactadherin are examples of protein-based phosphatidylserine (PS)-binding imaging agents [3–5]. Structural features of these agents can be generalized as including *1)* a binding site designed to accommodate the head group of a target phospholipid, and *2)* exposed hydrophobic side chains at the vicinity of the binding site for interacting with the core of the phospholipid bilayer. The first feature enables the recognition of phospholipid head groups, while the second provides an anchoring mechanism that drives toward membrane binding.

Duramycin, which is a lantibiotic peptide, also meets the structural criteria for targeting phospholipid membranes, but it binds specifically to phosphatidylethanolamine (PE) [6]. Apart from

apoptosis, emerging evidence indicates that the dynamics of membrane PE is involved in a number of biological functions, including cytokinesis and possibly hemostasis [7,8]. Thus, the unique binding activity of Duramycin adds to the repertoire of membrane-binding agents by enabling a new perspective in investigating the fundamental biology of membrane phospholipid distribution. Initial studies on ^{99m}Tc-labeled Duramycin indicate that the agent has good uptake in target tissues with rapid renal clearance and a low general background in vivo [9]. These properties are consistent with the structural features of Duramycin. More specifically, Duramycin is one of the smallest possible polypeptide (19 amino acids) that has a defined 3-dimensional binding structure [6,10]. The peptide is extensively cross-linked by intramolecular covalent bridges, thus exhibiting relatively high *in vivo* stability. The agent has binding activities comparable to large proteins, yet with peptide-like pharmacokinetics. The combination of these factors makes Duramycin an attractive candidate as an imaging agent for studying phospholipid distribution in the living system.

In light of these initial findings, the objective of the current study was to understand how ^{99m}Tc-Duramycin behaves in the target tissue, by quantifying the kinetics of interactions between ^{99m}Tc-Duramycin and its molecular targets *in vivo*. We hypothesize that the combination of high target density and fast probe diffusion in tissue will lead to more efficient uptake, thus superior imaging properties.

The in vivo experiment will be carried using a rat model of myocardial ischemia and reperfusion. It has been demonstrated that both PE and PS are externalized in dead and dying mammalian cells [11]. Additionally, extensive pathological data have documented that prolonged ischemia followed by reperfusion causes destabilization of sarcolemmal structure. Severe ischemic insult eventually leads to compromised phospholipid membrane integrity, rendering high levels of phosphatidylethanolamine accessible to extracellular agents [12–14]. The advantages of using this animal model include a relatively defined perfusion profile, high target density in the ischemically damaged myocardium versus a low background in the viable myocardium. The quantitative dynamic data acquired using this system, in turn, will help better define the utilities of ^{99m}Tc-Duramycin as a novel radiopharmaceutical. Importantly, this type of data will be

Nuclear Medicine and Biology, Vol. 39, No. 6 (August 2012): pg. 821-825. DOI.

instrumental in gauging the incremental values of an imaging agent compared with past and future generation agents for similar purposes.

MATERIALS AND METHODS

Radiolabeling of Duramycin

Duramycin and its partially inactivated form, Duramycin^{I}, were covalently modified with HYNIC. The molecular weight of the HYNIC-modified Duramycin was confirmed using Matrix-assisted laser desorption/ionization (MALDI) mass spectrometry. The radiopharmaceutical was prepared using a single-step kit formulation. The partially inactivated form of ^{99m}Tc-Duramycin was prepared in the same fashion. Quality control steps, including stability tests, were carried out as described before [11]. The radiopharmaceutical dose consistently has a radiochemical purity at 95% or greater, and is stable without significant presence of dissociated radioactivity.

Rat Model of Myocardial Ischemia and Reperfusion

The animal protocol was approved by the Institutional Animal Care and Use Committee under the NIH guideline. Male Sprague-Dawley rats were anesthetized with sodium pentobarbital (50 mg/kg) intraperitoneally. After tracheal intubation, respiration was maintained using a rodent ventilator. An incision was made between the 4th intercostal space to expose the heart. After opening the pericardium, the proximal left anterior descending coronary artery (LAD) was occluded for 30 minutes using a 6.0 suture at about 1 mm below the left atrial appendage. For sham operation, the suture was passed underneath the LAD without ligation. The presence of acute ischemia/reperfusion was confirmed by the pale appearance in the area-at-risk region and changes in ECG profiles. After reperfusion the chest wall was closed and ventilation was maintained until the rat could regain spontaneous respiration. The loose suture was left in place for area-at-risk staining.

SPECT studies

Static SPECT data were acquired at 40 min after radiotracer injection (37 MBq, i.v.) on a Triumph microSPECT/microCT scanner

(GE Healthcare, Waukesha, WI) equipped with a quad-detector SPECT system. The imaging parameters include multi-pinhole collimators for rat, 1.0 mm spatial resolution, 1100 counts per MBq sensitivity, 15% energy window centering at 140 keV, 50 × 50 mm trans-axial field of view, 170 mm axial field of view, 72 projections at 10 seconds each. SPECT acquisition was followed by CT, using the same field of view. The imaging data were reconstructed using the inbuilt software.

Spatial and Temporal uptake of ^{99m}Tc-Duramycin and its partially inactivated form in the area-at-risk

To investigate the temporal uptake kinetics of ^{99m}Tc-Duramycin in the area-at-risk, 20 rats were enrolled to simulate acute myocardial infarction with 30 min coronary occlusion as described above. At 2 hr after reperfusion the radiotracer was injected intravenously (0.1 mCi). One group of 4 rats was sacrificed for measurements at each of the following time points: 3, 10, 20, 60 and 180 min after injection. Immediately before sacrifice, a second thoracotomy was performed to expose the heart. The LAD was re-occluded at the same location by tightening the suture in place. Two mls of Evans Blue dye (2% w/v in PBS, pH 7.4) was infused into the tail vein. Area-at-risk was delineated by an absence of blue dye uptake, while the normally perfused myocardium is stained dark blue. The heart was quickly excised, and the dissected tissues were separately weighed and collected in sample tubes for gamma counting as follows: normal (blue), ischemic infarct (unstained). Three aliquots of ^{99m}Tc-Duramycin solution were taken at 5 ml each and were measured for radioactivity as standards for the calculation of total injected dosage (ID). The radioactivity uptake of ^{99m}Tc-Duramycin at each time point after injection was presented as percentage of injected dosage per gram (%ID/g) with standard deviation. The above studies were repeated in another group of 20 rats using the partially inactivated form of Duramycin.

Compartmental model

We modified a previously developed compartmental model for quantitative interpretation of the uptake kinetics of active and partially inactivated ^{9m}Tc-Duramycin in normal and infarct myocardium [17]. The model (Figure 1) consists a vascular region with volume V1 (ml)

representing the coronary circulation. For MI, the model allows ^{99m}Tc-Duramycin to participate in specific binding, where *B* is the amount (nmol) of free binding sited that are readily accessible to ^{99m}Tc-Duramycin at time t, and k_s (ml nmol^{-1} min^{-1}) is the association rate constant of ^{99m}Tc-Duramycin interaction with binding sites. For normal myocardial tissue, the model assumes that the binding sites are not accessible to ^{99m}Tc-Duramycin from the coronary circulation.

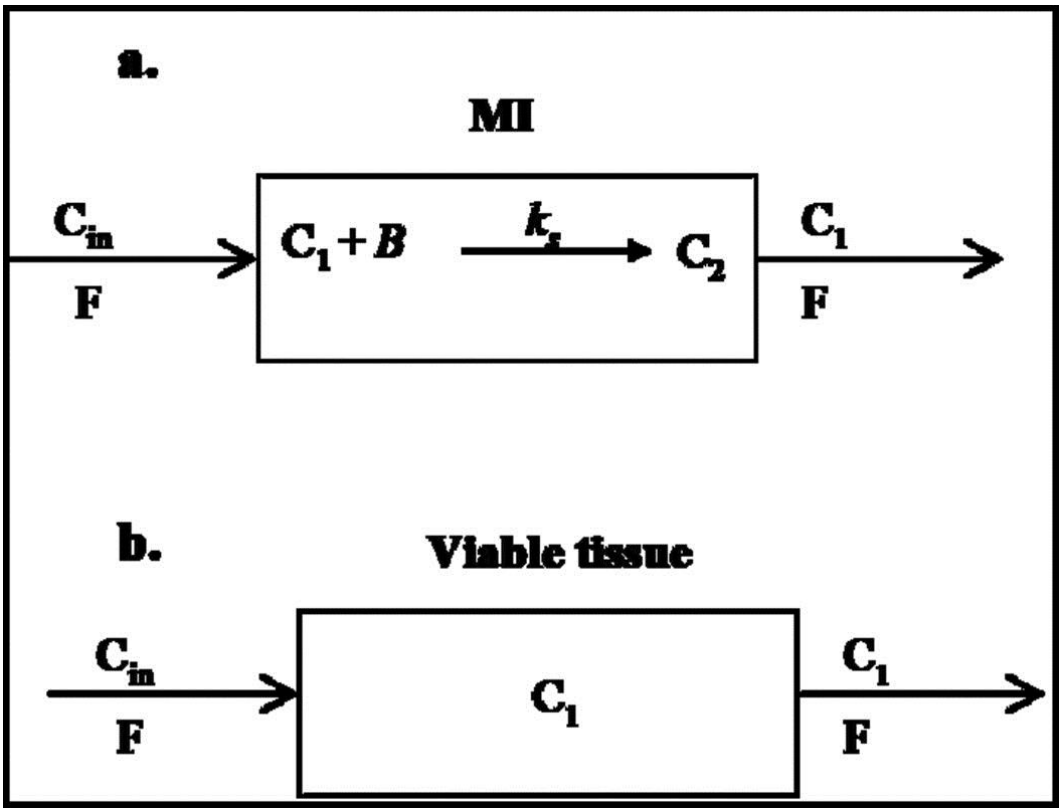

Figure 1 Compartmental model for the disposition of ^{99m}Tc-Duramycin in ischemic cardiac tissue (**a**.) and viable tissue (**b**.). $[C_1](t)$ is the probe concentration in the MI vascular region at time t; $C_2(t)$ is the amount of bound probe at time t. *B* is the amount of free receptors or binding sites at time t that is readily accessible for probe within the MI blood region; k_s is the probe-receptor association rate constant; F is the blood flow of the coronary circulation and $[C_{in}](t)$ is the input probe concentration for the coronary circulation.

Using mass balance and mass action, the temporal variations in the activities of free and bound ^{99m}Tc-Duramycin in V_1 are described by Equations (1–2)

Nuclear Medicine and Biology, Vol. 39, No. 6 (August 2012): pg. 821-825. DOI.

$$\frac{\mathrm{d}[\mathrm{C_1}]}{\mathrm{dt}} = \frac{\mathrm{F}}{\mathrm{V_1}}\Big([\mathrm{C_{in}}] - [\mathrm{C_1}]\Big) - \frac{-k_s}{\mathrm{V_1}}[\mathrm{C_1}]\Big(B_{\max} - \mathrm{C_2}\Big) \quad (1)$$

$$\frac{\mathrm{dC_2}}{\mathrm{dt}} = k_s[\mathrm{C_1}]\Big(B_{\max} - \mathrm{C_2}\Big), \quad (2)$$

where $[C_1](t)$ is the probe concentration (μM) in the MI vascular space at time t (t = 0 is probe injection time); $C_2(t)$ is the amount (nmol) of probe sequestered in the MI region via specific binding at time t; F is the blood flow of the coronary circulation (~ 1 ml min^{-1} g^{-1}); $[C_{in}](t)$ is the input probe concentration for the coronary circulation, which was estimated from previously measured ^{99m}Tc-Duramycin plasma clearance profile as described below; and B_{max} is the total amount (nmol) of readily accessible receptors or binding sites. The above equations are subject to the following initial (t = 0) conditions: [C1](t) = 0 μM, and $C_2(t)$ = 0 nmol. The total activated probe concentration at a given time t, $C_{total}(t)$ in %*ID* g^{-1} of tissue, in the system is

$$\mathrm{C_{total}(t)} = \frac{\big(\mathrm{V_1[C_1]} + \mathrm{C_2}\big)\big(MW10^{-7}\big)}{ID\,m}, \quad (3)$$

where *ID* (g) is the injected dose (~10 μg per 300 g rat); *m* (g) is the total mass of at-risk tissue (average 201 mg), and *MW* is the molecular weight of the radiopharmaceutical (3035 g mol^{-1}).

The model assumes that the partially inactivated form of ^{99m}Tc-Duramycin differs from the active form only in its affinity for the binding sites. Thus, the active and partially inactivated forms have the same B_{max}, V_1 and $[C_{in}](t)$, but different k_s values.

The governing differential equations for the disposition of ^{99m}Tc-Duramycin in normal myocardium reduce to Equation (1) with B_{max} set to zero. Thus, for normal myocardium, Equation (3) reduces to:

Nuclear Medicine and Biology, Vol. 39, No. 6 (August 2012): pg. 821-825. DOI.

$$C_{total}(t) = \frac{(V_1[C_1])(MW10^{-7})}{ID\,m} \quad (4)$$

Statistical comparisons were carried out using *t*-test or paired *t*-*test*, with $P < 0.05$ as the criterion for statistical significance.

RESULTS

Whole-body imaging

Whole-body SPECT images are shown in Figure 2. The high focal uptake of radioactivity is clearly seen in the ischemic myocardium in the tomographic images, which is made more conspicuous because of a lack of significant hepatic background. This is accompanied with a low systemic background and rapid renal/urinary clearance.

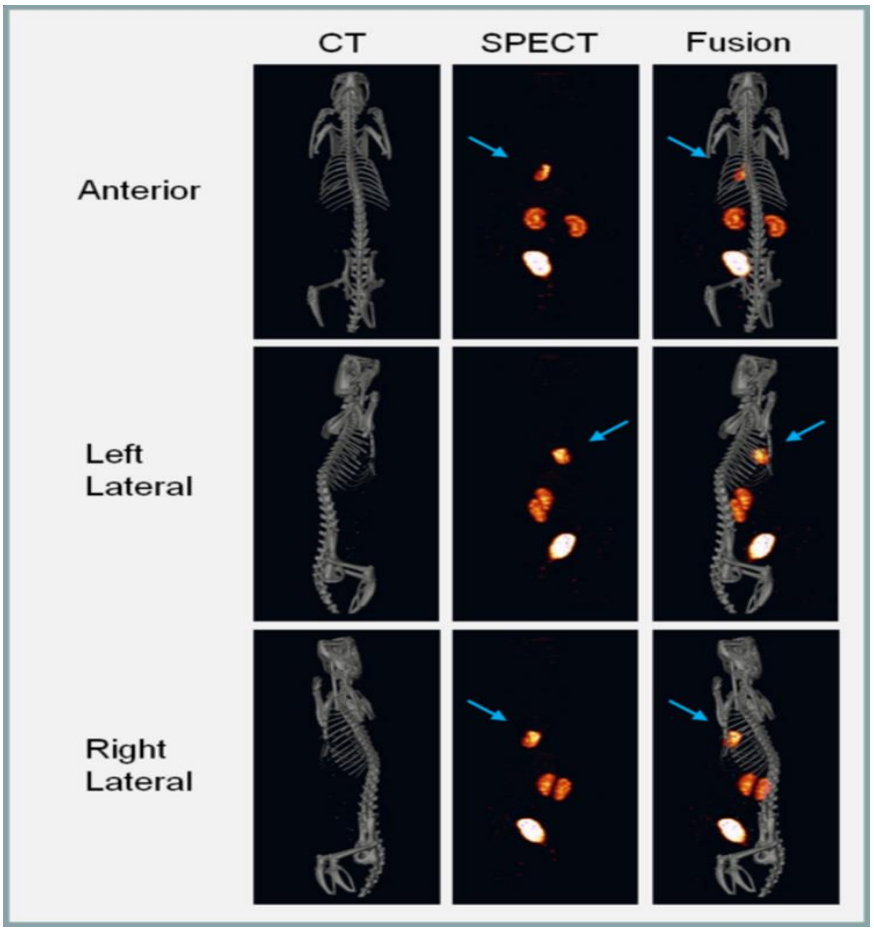

Nuclear Medicine and Biology, Vol. 39, No. 6 (August 2012): pg. 821-825. DOI.

Figure 2 Representative SPECT/CT images of ^{99m}Tc-Duramycin uptake in ischemically damaged cardiac tissue in vivo. The CT, SPECT and SPECT/CT fusion images are shown in the left, middle and right columns, respectively. Radioactivity uptake in the left ventricular free wall is highlighted with an arrow in the tomographic images.

Spatial and Temporal uptake of ^{99m}Tc-Duramycin in the area-at-risk

The uptake kinetics of ^{99m}Tc-Duramycin in the area-at-risk was characterized by measuring the level of radioactivity at different time points after injection and is summarized in Figure 3. Quantitative uptake data from dissected heart tissues of the infarct, and normal myocardium at 3, 10, 20, 60 and 180 min after tracer injection are presented. After injection the radioactivity uptake in the infarcted myocardium rapidly rose to 1.66 ± 1.18 (SD) %ID/g within 3 min, and approached a plateau by 10 min at 3.66 ± 0.76 %ID/g. The radioactivity uptake in the normal myocardium was low, reflecting the residual blood pool signal. According to the measurements using dissected heart tissues, at 60 min after injection, the average infarct-to-normal ratio was ~29. The radiotracer was sequestered in the irreversibly damaged myocardium, which is consistent with the high binding affinity and specificity of Duramycin-PE interactions. Chemical modification of a single amino acid (D15) resulted in a marked reduction in probe uptake (Figure 3).

Nuclear Medicine and Biology, Vol. 39, No. 6 (August 2012): pg. 821-825. DOI.

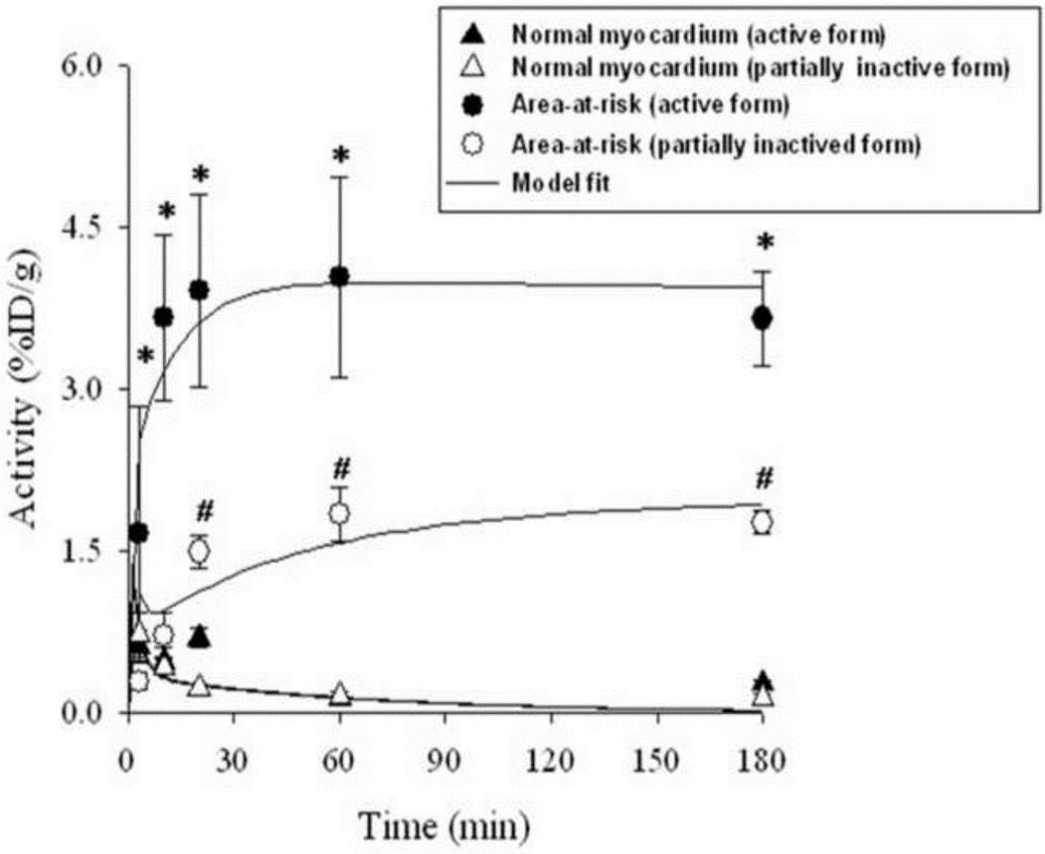

Figure 3 Kinetic analysis. Radioactivity uptake of the active and partially inactivated ^{99m}Tc-Duramycin, in terms of %ID/g, in ischemic and normal myocardium at 3, 10, 20, 60, and 180 min after intravenous injection. Values are mean ± SD. N = 4 for active and partially inactivated ^{99m}Tc-Duramycin at each of the time points. Solid lines are model fits. * Uptake of ^{99m}Tc-Duramycin in area-at-risk is significantly different from that for the partially inactivated ^{99m}Tc-Duramycin at the same time point ($P < 0.05$). # Uptake of partially inactivated ^{99m}Tc-Duramycin in area-at-risk is significantly different from its uptake in viable tissue at the same time ($P < 0.05$)

Kinetic analysis

The model parameters are V_1 (ml), the volume of the vascular region; B_{max} (nmol) the total amount of specific receptors or binding sites accessible to ^{99m}Tc-Duramycin in MI tissue; and k_s (ml nmol $^{-1}$ min^{-1}), the probe-receptor association rate constant. Estimation of these parameters was carried out as follows. First, $C_b(t)$, as *%ID*, was determined by fitting Equation (5) to previously measured ^{99m}Tc-Duramycin plasma clearance profile as a fraction of injected dose.

Nuclear Medicine and Biology, Vol. 39, No. 6 (August 2012): pg. 821-825. DOI.

$$C_b(t) = ae^{-\alpha 1 t} + be^{-\alpha 2 t} + (100 - a - b)e^{-\alpha 3 t}, \quad (5)$$

where a, b and (100 − a − b) are the amplitudes of the three exponentials with rate constants α_1 α_2, and α_3, respectively. The estimated values of the amplitudes *a* and *b* were 19.0 and 19.1 %ID, respectively. The estimated values of the rates constant α_1, α_2 and α_3 were 0.42, 0.02 and 0.42 min^{-1}, respectively, and the estimated half-life of the probe was 2.2 min.

Knowing $C_b(t)$, the input probe concentration for the coronary circulation, $[C_{in}](t)$ (in μM), was determined using

$$[C_{in}] = \frac{(C_b ID)10^9}{100 V_{in} MW}, \quad (6)$$

where V_{in} (ml) is the rat blood volume (~ 7% of total body weight).

Knowing [Cin](t), V1 (ml) was estimated by solving Equation (1) with *Bmax* = 0, and fitting Equation (4) to active or partially inactivated ^{99m}Tc-Duramycin activity versus time uptake data in normal myocardium (Figure 1). The estimated values of V1 from the active or partially inactivated ^{99m}Tc-Duramycin uptake data were virtually the same (Table 1). Knowing V_1, the remaining parameters namely, *Bmax*, and the association rate constant (k_s) for the active (k_{sa}) and partially inactivated (k_{si}) ^{99m}Tc-Duramycin were then estimated by solving Equations (1–2) with k_s set to k_{sa} or k_{si}, and fitting the resulting solutions of Equation (5) simultaneously to the active and partially inactive ^{99m}Tc-Duramycin uptake data in MI (Figure 3). The solid lines in Figure 3 demonstrate the ability of the model to fit the data.

Parameters	Estimated Values	95% confidence intervals
V_1 (ml) (active)	0.063	± 0.002
V_1 (ml) (partially inactivated)	0.060	± 0.009
B_{max} (nmol)	0.026	± 0.005
k_{sa} (ml nmol^{-1} min^{-1})	2.207	± 1.411
k_{si} (ml nmol^{-1} min^{-1})	0.259	± 0.135

Table 1 Estimated values and asymptotic confidence intervals of kinetic model parameters for ^{99m}Tc-Duramycin in area-at-risk

***k_{sa}*:** binding rate constant for ^{99m}Tc-Duramycin.

***k_{si}*:** binding rate constant for the partially inactivated ^{99m}Tc-Duramycin.

Table 1 shows the estimated values of the model parameters and measures of precision of these estimates, namely asymptotic 95% confidence intervals.

DISCUSSION

Significant findings from the current investigation include the follows: *i)* ^{99m}Tc-Duramycin has rapid uptake in the target tissue, presumably in a PE-dependent manner. Once bound, there is minimal washout over extended period of time. *ii)* The binding kinetics of ^{99m}Tc-Duramycin is quantitatively analyzed, where these values allow an in-depth understanding of the strength and limitations of this imaging agent. An added benefit is that the availability of quantitative kinetic data enables an assessment of incremental values and for guiding the development of future generation agents. The current findings are discussed in more details as follows.

Cognate interactions between the probe and binding target are dependent on the accessibility of these targets to probe from the vascular region. Smaller probes tend to have a greater tissue

permeability, which leads to a more efficient target access. To date, a phospholipid-binding agent other than ^{99m}Tc-Duramycin with established quantitative kinetic data is ^{99m}Tc-C2A-GST. Comparatively, probe's tissue permeability was a limiting factor for ^{99m}Tc-C2A-GST, but not for ^{99m}Tc-Duramycin, in part due to its much lower molecular weight.

Using kinetic analysis, we were able to estimate the binding rate constant for ^{99m}Tc-Duramycin in the target tissue. This value reflects the binding affinity of the agent in the actual tissue settings. The availability of the in vivo binding rate constant enables comparative studies that are free from extrapolations based on binding constants obtained from in vitro binding assays. According to the current study, the binding rate constant (k_s) for ^{99m}Tc-Duramycin is comparable than that of ^{99m}Tc-C2A-GST (Table 2) [13]. Quantitative analysis indicates that covalent modification of D15, which forms a portion of Duramycin binding pocket, resulted in a substantial decrease in binding rate constant. This is indicative that the uptake of ^{99m}Tc-Duramycin is indeed PE dependent.

Parameters	^{99m}Tc-Duramycin	^{99m}Tc-C2A-GST
V_1 (ml g^{-1})	0.31	0.24
B_{max} (nmol g^{-1})	0.13	0.05
k_{sa} (ml nmol^{-1} min^{-1})	2.21	2.32
Plasma half life (min)	2.2	10.0

Table 2 Comparison of values of model parameters descriptive of the uptake of ^{99m}Tc-Duramycin and ^{99m}Tc-C2A-GST in area-at-risk

V_1 and B_{max} are normalized to mass of at-risk tissue. k_{sa} is binding rate constant for ^{99m}Tc-Duramycin.

In terms of total binding capacity (B_{max}), this is a parameter that is intrinsic to the target tissue, and is a measure of the available binding sites for a given probe. By comparing the kinetics between ^{99m}Tc-Duramycin and ^{99m}Tc-C2A-GST, two membrane-binding agents that differ from structural properties to binding targets, it provides a unique opportunity to look at the total binding capacity from two independent angles. According to the kinetic analysis results, the B_{max}

(nmol/g) for ^{99m}Tc-Duramycin, which is the density of available PE, is about 3-fold greater than that of ^{99m}Tc-C2A-GST (Table 2), which is the density of available PS [13]. This outcome is consistent with the published values of PE/PS ratio from cellular membranes [14]. It is indicative that the molecular targets, PE and PS, are constituents of a single pool of membrane phospholipids exposed in dead and dying cells. A significant point of the current study, therefore, is that the underlying pathophysiology is a constant beyond the variability of different imaging agents or their targets.

The ~3-fold difference in the number of available binding sites for ^{99m}Tc-Duramycin as compared to ^{99m}Tc-C2A-GST resulted in only ~50% increase in the uptake of ^{99m}Tc-Duramycin in MI at steady state as compared to ^{99m}Tc-C2A-GST [13]. This result is in part due to the faster blood clearance rate of ^{99m}Tc-C2A-GST as compared to ^{99m}Tc-C2A-GST (Table 2). This stresses the importance of the above kinetic modeling approach for the quantitative interpretation of ^{99m}Tc-Duramycin kinetic data since the 3-fold difference in the number of available binding sites cannot be predicted directly from the kinetic data without accounting for the contributions of the other factors that determine the uptake kinetics of ^{99m}Tc-Duramycin in MI, including blood clearance rate, probe tissue permeability, and probe-target binding rate constant.

In terms of potential impact on patient care, current clinical radiotracers are valuable in providing perfusion, functional and metabolic information on target tissues, such as the heart; however, there lacks a positive imaging agent for detecting active cell death in degenerative diseases. A targeted radiotracer that binds externalized phospholipids as a surrogate marker for cell death will aid the early detection of tissue injury and the monitoring of the efficacy of therapeutic interventions.

Overall, in a quantitative approach, we have characterized the in vivo behaviors of ^{99m}Tc-Duramycin in the target tissue. The relatively high target-to-background ratio is due to a combination of the following factors: enhanced tissue permeability, site-directed radiolabeling, prompt blood clearance, and a greater target density.

Nuclear Medicine and Biology, Vol. 39, No. 6 (August 2012): pg. 821-825. DOI.

ACKNOWLEDGMENTS

The authors are grateful to C. M. O'Connor, M.A., for editorial help. Technical assistance of Dr. Xiaoguang Zhu is greatly appreciated. This work was supported in part by the American Heart Association (0435147N) and the National Institutes of Health (1R01HL102085, 1S10RR027540, and HL-24349), and the Department of Veterans' Affairs.

Footnotes

REFERENCES

1. Yamaji-Hasegawa A, Tsujimoto M. Asymmetric distribution of phospholipids in biomembranes. Biol Pharm Bull. 2006;29:1547–1553.

2. van Meer G, Voelker DR, Feigenson GW. Membrane lipids: where they are and how they behave. Nat Rev Mol Cell Biol. 2008;9:112–124.

3. Blankenberg FG, Katsikis PD, Tait JF, Davis RE, Naumovski L, Ohtsuki K, Kopiwoda S, Abrams MJ, Darkes M, Robbins RC, Maecker HT, Strauss HW. In vivo detection and imaging of phosphatidylserine expression during programmed cell death. Proc Natl Acad Sci USA. 1998;95:6349–54.

4. Zhao M, Beauregard DA, Loizou L, Brindle KM. Non-invasive detection of apoptosis using magnetic resonance imaging and a targeted contrast agent. Nat Med. 2001;7:1241–44. [

5. Waehrens LN, Heegaard CW, Gilbert GE, Rasmussen JT. Bovine lactadherin as a calcium-independent imaging agent of phosphatidylserine expressed on the surface of apoptotic HeLa cells. J Histochem Cytochem. 2009;57:907–914.

6. Hayashi F, Nagashima K, Terui Y, Kawamura Y, Matsumoto K, Itazaki H. The structure of PA48009: the revised structure of duramycin. J Antibiot (Tokyo) 1990;43:1421–1430.

7. Emoto K, Inadome H, Kanaho Y, Narumiya S, Umeda M. Local change in phospholipid composition at the cleavage furrow is essential for completion of cytokinesis. J Biol Chem. 2005;280:37901–37907.

8. Li Z, Wells CW, Esmon CT, Zhao M. Phosphatidylethanolamine at the endothelial surface of aortic flow dividers. J Thromb Haemost. 2009;7:227–229.

9. Zhao M, Li Z, Bugenhagen S. ^{99m}Tc-labeled duramycin as a novel hosphatidylethanolamine-binding molecular probe. J Nucl Med. 2008;49:1345–1352.

10. Zimmermann N, Freund S, Fredenhagen A, Jung G. Solution structures of the lantibiotics duramycin B and C. Eur J Biochem. 1993;216:419–428.

11. Emoto K, Toyama-Sorimachi N, Karasuyama H, Inoue K, Umeda M. Exposure of phosphatidylethanolamine on the surface of apoptotic cells. Exp Cell Res. 1997;232:430–434.

12. Farb A, Kolodgie FD, Jenkins M, Virmani R. Myocardial infarct extension during reperfusion after coronary artery occlusion: pathologic evidence. J Am Coll Cardiol. 1993;21:1245–1253.

13. Post JA, Bijvelt JJ, Verkleij AJ. Phosphatidylethanolamine and sarcolemmal damage during ischemia or metabolic inhibition of heart myocytes. Am J Physiol. 1995;268:H773–780.

14. Post JA, Verkleij AJ, Langer GA. Organization and function of sarcolemmal phospholipids in control and ischemic/reperfused cardiomyocytes. J Mol Cell Cardiol. 1995;27:749–760.

15. Edwards DS, Liu S, Barrett JA, et al. New and versatile ternary ligand system for technetium radiopharmaceuticals: water soluble phosphines and tricine as coligands in labeling a hydrazinonicotinamide-modified cyclic glycoprotein IIb/IIIa receptor antagonist with ^{99m}Tc. Bioconjug Chem. 1997;8:146–154.

16. Liu S, Edwards DS, Barrett JA. ^{99m}Tc labeling of highly potent small peptides. Bioconjug Chem. 1997;8:621–636.

17. Audi S, Poellmann M, Zhu X, Li Z, Zhao M. Quantitative Analysis Of ^{99m}Tc-C2A-GST Distribution In The Area-At-Risk After Myocardial Ischemia And Reperfusion Using A Compartmental Model. Nucl Med Biol. 2007;34:897–905.

18. Post JA, Langer GA, Op den Kamp JA, Verkleij AJ. Phospholipid asymmetry in cardiac sarcolemma. Analysis of intact cells and 'gas-dissected' membranes. Biochim Biophys Acta. 1988;943:256–266.

About the Authors

Ming Zhao: Feinberg Cardiovascular Research Institute, Department of Medicine, Northwestern University, 303 E. Chicago Avenue, Tarry 14-753, Chicago, Il, 60611.

Email: m-zhao@northwestern.edu

Phone: 312-503-3226